Nonlinear MHD Dynamics Of Tokamak Plasmas On Multiple Time Scales

S.E. Kruger 1), D.D. Schnack 1), D.P. Brennan 2), T.A. Gianakon 3), C.R. Sovinec 4)

1) SAIC, San Diego, California, USA
2) General Atomics, San Diego, California, USA
3) Los Alamos National Laboratory, Los Alamos, New Mexico, USA
4) University of Wisconsin-Madison, Madison, Wisconsin, USA

email contact: krugers@saic.com

Abstract. Two types of numerical, nonlinear simulations using the NIMROD code are presented. In the first simulation, we model the disruption occurring in DIII-D discharge 87009 as an ideal MHD instability driven unstable by neutral-beam heating. The mode grows faster than exponential, but on a time scale that is a hybrid of the heating rate and the ideal MHD growth rate as predicted by analytic theory. The second type of simulations,which occur on a much longer time scale, focus on the seeding of tearing modes by sawteeth. Pressure effects play a role both in the exterior region solutions and in the neoclassical drive terms. The results of both simulations are reviewed and their implications for experimental analysis is discussed.

Long wavelength instabilities in fusion plasmas have often been described within the framework of magnetohydrodynamic (MHD) theory. These instabilities are often categorized by the physics in the generalized Ohm's law required for the instability to be described (e.g. ideal, resistive, neoclassical). The types of instabilities have different time scales associated with their growth, with the ideal modes growing on the Alfvenic time scale, and the other modes having a time scale that is a hybrid of the Alfvenic and resistive time scales. For both types of instabilities, understanding the mode onset is crucial for predicting the operational limits of future devices.

Recently, an analytic theory [1]has been put forth to describe the growth of an instability being driven through the marginal point. Assuming that the free energy of the mode is proportional to β; $\omega^2 = \delta W/\delta K \sim -\hat{\gamma}^2_{MHD}\,(\beta/\beta_{crit} - 1)$; and approximating the heating as a linear increase in β with a heating rate γ_h near the marginal point; $\beta(t) = \beta_{crit}(1+\gamma_h t)$; one obtains that the resultant mode grows with a faster-than-exponential rate:

$$\xi = \xi_0 \exp\left[(t/\tau)^{3/2}\right]. \tag{1}$$

The time constant of the mode is a hybrid of the variation of the growth rate with beta and the heating time scale:

$$\tau \equiv \frac{(3/2)^{2/3}}{(\hat{\gamma}_{MHD})^{2/3}\gamma_h^{1/3}}. \tag{2}$$

As the limit of either $\hat{\gamma}_{MHD}$ or γ_h go to zero, the mode does not grow because it is exactly at the marginal point.

1 Fast-time scale simulations

The heuristic analytic theory of the previous section was successfully used to explain many of the features of DIII-D discharge 87009 which disrupted during neutral-beam heating. [1]To further test this theory and gain additional insight into the nonlinear behavior, we have modeled discharge 87009 with an equilibrium with similar pressure and safety factor profiles as the actual discharge at 1681.7 msec, but with the plasma pressure raised to the marginal stability point when a conducting wall is placed on the last closed flux surface.

To model the heating of the plasma, we apply a heating source that increases the equilibrium pressure self-similarly $\frac{\partial p}{\partial t} = ... + \gamma_h p_{eq}$. As the plasma heats, the flux surfaces will shift outward, but the heating will still be peaked at the old magnetic axis. Because our heating rate will be slow compared to the growth of the mode, but still much faster than the resistive decay time ($\hat{\gamma}_{MHD} \gg \gamma_h \gg 1/\tau_R$), we satisfy the assumptions of the analytic theory. Note that throughout the simulations, NIMROD's finite-element grid which is aligned to the equilibrium magnetic field does not move.

The NIMROD simulations were run with Lundquist number, $S = 10^6$, Prandtl number (ratio of normalized resistivity to kinematic viscosity) $Pr = 200$ with heating rates of $\gamma_h = 10^{-3}\ s^{-1}$ and $\gamma_h = 10^{-2}\ s^{-1}$. A finite-element grid in the poloidal plane with 128 radial vertexes and 64 poloidal vertexes were used with cubic polynomial Lagrangian elements. The toroidal direction is discretized using the pseudo-spectral method with the $n = 0$ and $n = 1$ modes kept. The results of a NIMROD simulations with $\gamma_h = 10^{-3}\ s^{-1}$ are shown in Figure 1a, and the fits for both heating rates are shown in Figure 1b. As predicted by the analytic theory, the growth of the mode is faster than exponential as represented by the straight lines in Figure 1b. The slight difference between the two heating rates is believed to be due to the fact that we actually start slightly above the marginal stability point and due to non-ideal effects. Fitting the results to the exponential growth given by Eq. (1), gives a fit to the time constant of $\tau \sim \hat{\gamma}_{MHD}^{-0.72} \gamma_h^{-0.28}$ which agrees well with the analytic prediction given by Eq. (2). Unlike internal kinks, which can often saturate at small amplitudes with

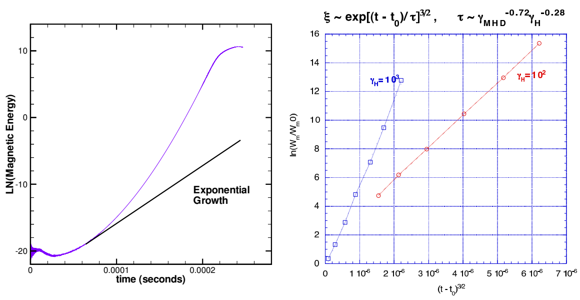

Figure 1: In 1a (left), the mode clearly grows faster than exponential. In 1b (right), both heating rates give good fits to the scaling of Eq. (1) as shown by the straight lines.

current sheets, [2], or tearing modes, that are discussed in the next section, these nonlinear instabilities have both robust growth and no loss of confinement as they enter into the nonlinear stage; an observation consistent with experimental observations.

2 Slow-time scale simulations

Unlike the interchange-parity modes observed in the previous case, tearing modes break field lines at all amplitudes causing significant loss of confinement even though their saturated amplitudes and growth rates are smaller. The seeding mechanisms of such modes remain poorly understood [3]and remain a critical unsolved problem for prediction of future reactors. In this paper, we consider the self-consistent generation of tearing modes by $1/1$ sawteeth within the context of strictly fluid models. Because we use only fluid models, have the conducting wall on the last closed flux surface, and have no shear flow, these simulations are limited. However, because we use exact equilibrium reconstructions and run at relatively large Lundquist numbers, these are important steps in gaining a full understanding of how these modes arise in experiments.

DIII-D discharge 86166 is an ITER-like long-pulse experiment which observes a series of sawtooth events and the eventual emergence of a $m/n = 3/2$ tearing mode which causes confinement degradation. Because the beam power is constant throughout the time sequence shown, and there is relatively little variation in plasma parameters, the emergence of the $3/2$ mode after a series of nearly identical sawteeth has been a mystery. Recently, a theory has been put forth [4]which explains the triggering of the $3/2$ mode as being classically driven due to a sharp increase in Δ' when the plasma is near an ideal MHD stability boundary.

To test the theory, equilibria were obtained from two time slices, $t = 2990\ msec$ and $t = 3600\ msec$. The primary difference between these two equilibria is in the pressure profiles. For the simulations presented in this section, a resistive MHD model is used with a Lundquist number $S = 2.4 \times 10^6$ and a Prandtl number $Pr = 1000$. A comparison of the mode growths for the two cases is shown in Figure 2. In both cases, the initial mode perturbation is due to a $1/1$ mode. As the mode becomes larger, the $n = 2$ mode is driven nonlinearly as can be clearly seen from the slope of the $n = 2$ curve being twice that of the $n = 1$ curve. After being nonlinearly driven, the $n = 2$ mode from the earlier case decays, while the $t = 3600$ case continues to grow. To match to experiment, we plan on using neoclassical closures.

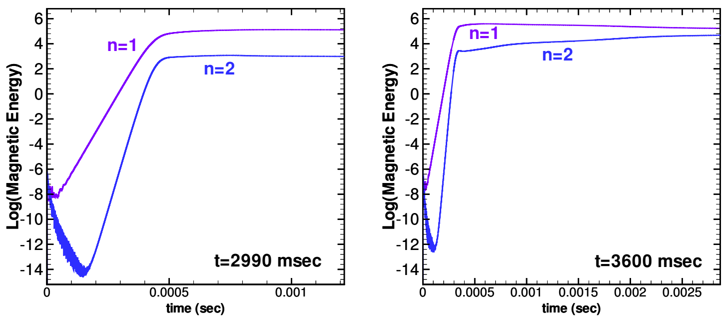

Figure 2: Despite similar equilibria, the $m/n = 3/2$ island grows in the later discharge after the sawtooth.

Recently, a heuristic closure was developed [5]to improve previous forms. The closure gives as the divergence of the stress tensor for each species α

$$\vec{\nabla} \cdot \Pi_\alpha = \rho_\alpha \mu_\alpha \left\langle B^2 \right\rangle \frac{\vec{V}_\alpha \cdot \vec{e}_\Theta}{\left(\vec{B} \cdot \vec{e}_\Theta\right)^2} \vec{e}_\Theta, \tag{3}$$

where the viscous damping coefficient, μ_α, contains information about the magnetic geometry and particle trapping and $\vec{e}_\Theta$ is a unit vector in the poloidal direction. This closure improves previous numerical closures because in addition to the perturbed bootstrap current drive, it includes the physics of enhanced polarization current, neoclassical enhancement of the resistivity, and poloidal flow damping. Furthermore, this closure is entropy-producing when averaged over the plasma volume and is relatively easy to implement. This closure has been well-benchmarked [5]and is successful in reproducing the analytic stability boundary as seen in Fig. 3.

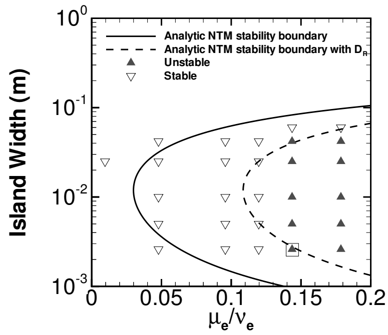

Figure 3: The heuristic closure numerically reproduces the stability boundary expected from analytic theory.

To test the closure on an experimental case to determine if it can give quantitative description of the growth of a $m/n = 3/2$ mode in DIII-D discharges, we examine DIII-D discharge 86144 which is similar to the discharge 86166 described above. As in the previous simulations, we are trying to understand the onset mechanisms of this mode. We first investigate the nonlinear coupling of this mode. Numerical results show that as the Lundquist number increases, the generated island decreases as predicted by analytic theory [6]

Simulating neoclassical tearing modes requires sufficient pressure flattening in the vicinity of the island. Finite perpendicular diffusivity gives a threshold island width that scales as $W_d \sim \left(\chi_\perp / \chi_{||}\right)^{1/4}$. [7]For the mode to grow, sufficiently large parallel thermal diffusivity is needed to overcome this threshold. To match the same asymptotic regime as the experiment, scale length of the thermal diffusivity anisotropy needs to be greater than the visco-resistive layer width ($W_d > \delta_V$), [8]which implies that the simulations need to be run at large Lundquist number. This decreases the generated island size which implies that we need to have have a larger parallel thermal diffusivity to lower the threshold. As pointed out in Ref. [8],this implies that the simulations need to operate at same plasma parameters as the experiment. We show the results of the simulations of DIII-D discharge 86144 in Figure 4. To date, we have not had the island grow to the experimentally observed island size of $\sim 6 - 10\ cm$.

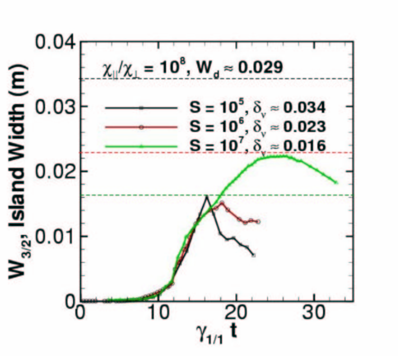

Figure 4: Simulations of DIII-D discharge 86144 show sensitivity to the diffusivities used in the simulations.

3 Discussion and Conclusions

NIMROD simulations of DIII-D discharges have focused on two types of discharges, a fast-time scale instability which is believed to have caused a disruption, and the seeding of slow-time scale tearing modes. The simulations have several goals in common: a self-consistent description of how the plasma reaches the unstable state, the need for running simulations at realistic plasma parameters, and the importance of mode coupling in interpreting the results.

The ability to routinely run simulations of tokamak discharges at realistic values of diffusivities (kinetic, electrical, and thermal) has greatly increased the power of these calculations in making experimental comparisons and in being able to operate near the marginal stability point. As the NIMROD project continues to develop and evolve, we expect that the ability to routinely include additional physics; such as shear flow, the vacuum region, two fluid effects, and kinetic closures, will both greatly increase the ability to make quantitative comparisons, and rapidly increase the computational resources required.

References

[1] J. Callen et.al., Phys. Plasmas, 6 (1999), 2963.
[2] M. Rosenbluth, R. Dagazian, and P. Rutherford, Phys. Fluids, 16 (1973),1894.
[3] J. Connor, F. Waelbroeck, and H. Wilson, Phys. Plasmas, 8 (2001), p. 2835.
[4] D. Brennan et.al, Phys. Plasmas, 9 (2002), 2998.
[5] T. Gianakon, S. Kruger, and C. Hegna, Phys. Plasmas, 9 (2002), 536.
[6] C. Hegna, J. Callen, and R. LaHaye, Phys. Plasmas, 6 (1999), 130.
[7] R. Fitzpatrick, Phys. Plasmas, 2 (1995), p. 825.
[8] H. Lutjens, J. L. A. Bondeson, and X. Garbet, Phys. Plasmas, 9 (2002),219.